Comparative Medicine
Copyright 2019
by the American Association for Laboratory Animal Science

Vol 69, No 1
February 2019
Pages 48–54

Original Research

Factors Affecting Growth Kinetics and Spontaneous Metastasis in the B16F10 Syngeneic Murine Melanoma Model

Natalie Fowlkes, Kelli Clemons, Paul JF Rider, Ramesh Subramanian, Nobuko Wakamatsu, Ingeborg Langohr, and Konstantin G Kousoulas*

Melanoma is an immunogenic tumor that can metastasize quickly to proximal and distal sites, thus complicating the application of therapeutic modalities. Numerous mouse model systems have been used to gain understanding of the immunobiology and metastatic potential of melanoma. Here, we report the optimization of a syngeneic mouse melanoma model protocol using the mouse B16-derived melanoma cell line B16F10 that ensures the production of tumors on mice pinnae that are similar in size between animals and that enlarge in a time-dependent manner. In this model, B16F10 cells are first allowed to develop tumors after injection in the interscapular area or flank of C57BL/6J mice. Subsequently, the tumors are harvested, cells dissociated and injected into mouse pinnae. Dose-dependent studies revealed that injection of 2×10^5 cells allowed for slow tumor enlargement, producing tumors averaging 100 mm^3 within 2 to 3 wk with a metastatic frequency of 100%. This experimental protocol will be useful in dissecting the immunobiology of melanoma tumor development and metastasis and the evaluation of immunotherapeutic antimelanoma therapies.

DOI: 10.30802/AALAS-CM-18-000036

Melanoma is the sixth most common type of cancer overall in humans, and its incidence has been increasing yearly in the United States for the last 30 y. When cutaneous melanoma is diagnosed at an early stage, patients can be cured through surgical excision of the tumor and can expect 5-y survival rates as high as 97%. However, at least 13% of melanoma patients already have metastasis to regional or distant sites by the time they are diagnosed with the disease. The most common first site of melanoma metastasis is the sentinel lymph node (that is, the first lymph node to which cancer cells are most likely to spread from a primary tumor), and numerous studies have shown that status of this lymph node reflects that of the entire topography of regional lymph nodes.[7,8,14,20]

Metastasis is a significant problem in the treatment of cancer, accounting for more than 90% of cancer-related deaths in people.[9] Treatment options for while metastatic melanoma in human patients particularly have been limited because metastatic melanoma is resistant to most traditional cancer therapies. Efforts to improve the efficacy of novel treatment strategies and minimize the incidence of adverse events are ongoing in clinical trials. In many cases, these trials are occurring in advance of the preclinical studies that are intended to support them.[18] In other cases, preclinical studies were performed and showed promising results in the laboratory, but therapeutic benefit failed to translate to human clinical trials. The lack of appropriate models for thorough preclinical testing of treatment strategies is often blamed for these failures.[3]

Received: 27 Mar 2018. Revision requested: 05 May 2018. Accepted: 10 Jun 2018.
Department of Pathobiological Sciences, School of Veterinary Medicine, Louisiana State University, Skip Bertman Drive, Baton Rouge, Louisiana
**Corresponding author. Email: vtgusk@lsu.edu*

The metastatic behavior of melanoma is a specific challenge in murine tumor modeling. Typically, an experimental metastasis model involves direct injection of neoplastic cells into the bloodstream, most commonly into the tail vein of mice. Pulmonary nodules resulting from intravenous injection are frequently referred to as metastases; however, intravenous injection leads to the production of a multitude of de novo tumors, because key steps in the metastatic cascade, including invasion into the tissue, detachment, and migration into the vasculature (intravasation), are bypassed completely.[21] In contrast, spontaneously metastasizing models allow the entire metastatic cascade to be modeled from invasion to colonization of distant sites.[13] In addition, spontaneously metastasizing models allow meaningful comparison of differences in protein or gene expression or immune cell infiltration between primary and metastatic lesions.

The B16 cell line is the most widely used line for melanoma research due to its aggressive growth, and it remains the standard in the field for the development of immunotherapies for melanoma.[21,28] Nonetheless, the B16 melanoma line does not typically form spontaneous metastases after subcutaneous implantation.[17] To simulate pulmonary metastasis with this model, B16F10 cells are typically injected into the tail vein in an acute experimental metastasis model, as mentioned previously.[21] Loss of the metastatic phenotype may in part be related to years of maintenance in vitro.[6] In addition, changes in the inoculation site can often alter tumor growth characteristics.[19,25,26] Protocols that establish consistent growth and predictable, spontaneous metastasis in robust murine tumor models are therefore greatly needed in cancer drug development for early preclinical studies. Here, we describe a C57BL/6J/B16F10 mouse melanoma protocol that allows for the development of B16F10 tumors on

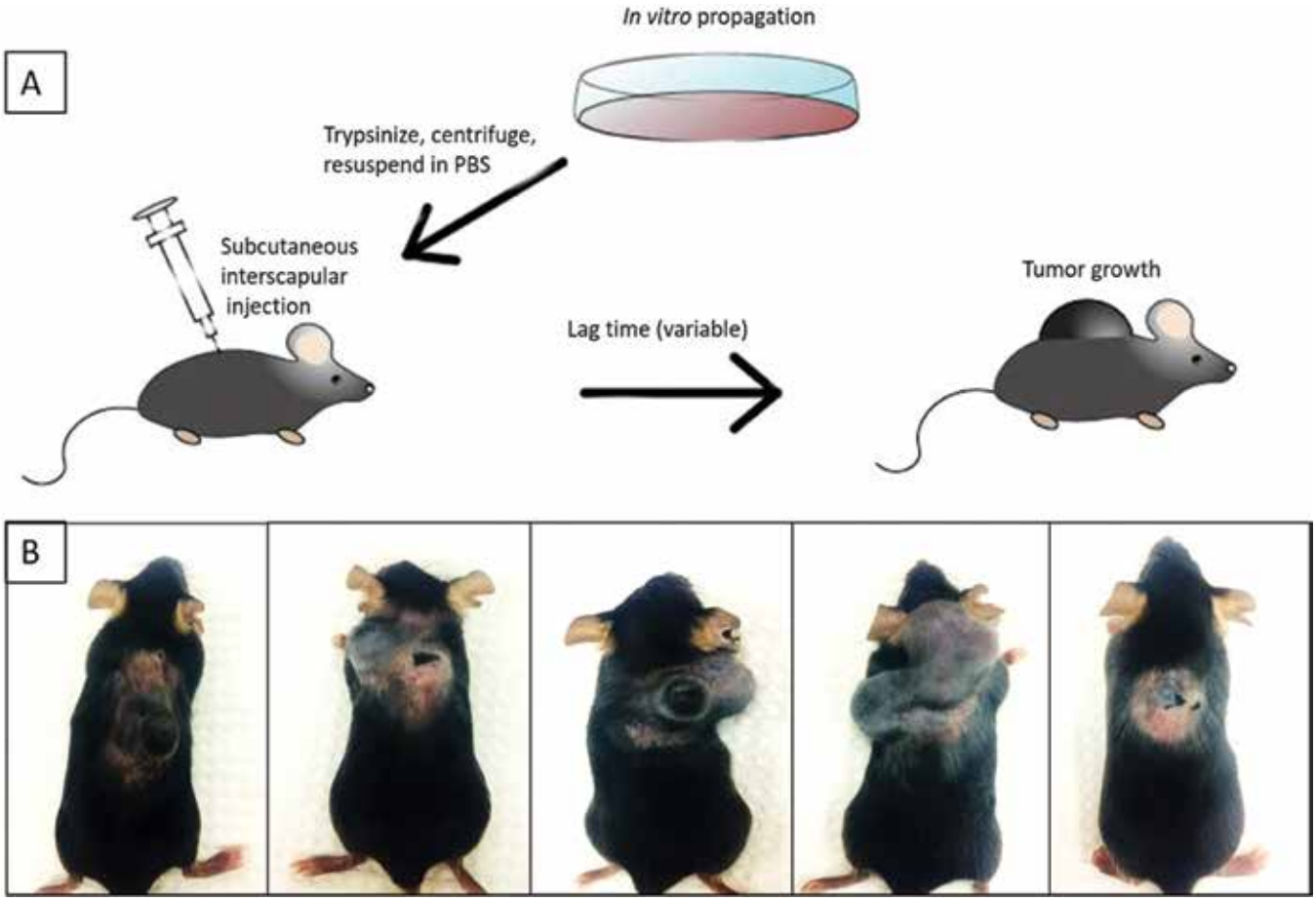

Figure 1. (A) Schematic demonstrating a typical engraftment protocol in the B16F10 murine melanoma model. (B) Subcutaneous B16F10 melanoma tumors in the interscapular region at 2 wk after engraftment. Engraftment of B16F10 cells in this location results in variable tumor morphology and growth in C57BL/6J mice.

mouse pinna that are similar in size between animals after initial engraftment in mouse interscapular or flank areas. This model allows for the development of sizeable tumors within 2 to 3 wk and efficient metastasis to regional lymph nodes.

Materials and Methods

Animals. Female C57BL/6J female mice (age, 6 to 8 wk) were purchased from the Jackson Laboratory (Bar Harbor, ME). Animals were acclimated for at least 3 d prior to experimental use. Mice were identified by using ear tags in the right pinna. Animals were housed under standard conditions with no more than 5 per cage. Mice were housed in ventilated, filter-top cages containing corncob bedding (catalog 7097, 1/4-in., Teklad, Envigo, Somerset, NJ) and were maintained on a 12:12-h light:dark cycle at 22 ± 2 °C. Enrichment was provided in the form of social housing and cotton nesting material. Mice had free access to chow (no. 5001, LabDiet, St Louis, MO) and tap water. Animals were maintained in accordance with the *Guide for the Care and Use of Laboratory Animals*[12] in an AAALAC-accredited facility. All procedures were approved by the Louisiana State University IACUC and followed applicable governmental policies and regulations.

Cell culture propagation. B16F10 murine melanoma cells were obtained from American Type Culture Collection (Vienna, VA), maintained under sterile conditions at 37 °C with 5% CO_2, and propagated as adherent monolayers in T75 flasks containing DMEM supplemented with 10% filtered, heat inactivated FBS and 100 µg/mL Primocin (Invivogen, San Diego, CA). Prior to use, cells were trypsinized, centrifuged, counted by using a hemocytometer, and resuspended to the desired concentration in sterile PBS. Trypan blue exclusion was performed to evaluate cell viability during counting; cell viability was at least 90% for all experiments.

In vivo propagation. After shaving of the skin and disinfection by using a 70% isopropyl alcohol-soaked gauze, 3 C57BL/6J female mice were injected with 2×10^6 early-passage B16F10 cells suspended in 100 µL PBS in the interscapular subcutis. A 1-mL syringe with a 27-gauge needle was used for injections. Subcutaneous engraftment occurred while animals were anesthetized with 2% to 3% isoflurane. At 10 to 14 d, mice were euthanized, and tumors (diameter, 1 to 1.5 cm) were processed for pinna engraftment in additional mice. Tumors were isolated, placed in a sterile culture dish, minced by using a scalpel blade, and placed in an incubator at 37 °C with 5% CO_2 with 3 mL of trypsin for approximately 20 min. Cells were strained through a 40-µm strainer, and complete DMEM with 100 µg/mL Primocin was added before counting on a hemocytometer and evaluating for viability by using trypan blue exclusion; cell viability was 90% or greater for experiments. Cells were centrifuged and resuspended in PBS at concentrations of 2×10^6 and 4×10^6 cells/mL and placed on ice for transportation and pinna engraftment within 1 h of harvesting.

Pinna engraftment. Mice were anesthetized with 2% to 3% isoflurane, and B16F10 cells were engrafted orthotopically in the dermis of the dorsal left dorsal pinna, which had been disinfected by using 70% isopropyl alcohol; a 1-mL syringe with a

Table 1. Comparison of tumor growth and metastasis in B16F10-bearing mice according to the number of cells inoculated

No. of B16F10 cells inoculated	No. of mice with tumors/ total no. of mice (%)	No. of mice with metastasis/ total no. of mice with tumors (%)	Lag time (d)	Overall survival (d)	Duration of disease (d)	Tumor volume at detection (mm^3)	Tumor volume at euthanasia (mm^3)
2×10^5	10/11 (91%)	10/10 (100%)	21 ± 0	27.1 ± 1.4[a,b]	6.1 ± 1.441	114.0 ± 48.7	481.7 ± 104.7
4×10^5	17/17 (100%)	9/17 (53%)	8.1 ± 0.7[c,d]	15.8 ± 0.5	6.8 ± 0.8	130.3 ± 43.7	765.7 ± 135.3

Data are given as mean ± SEM, where appropriate.
[a]$P < 0.0001$ (unpaired *t* test, parametric, 2-tailed)
[b]$P = 0.0026$ (F test to compare variances)
[c]$P < 0.0001$ (unpaired *t* test, parametric, 2-tailed)
[d]$P < 0.001$(F test to compare variances)

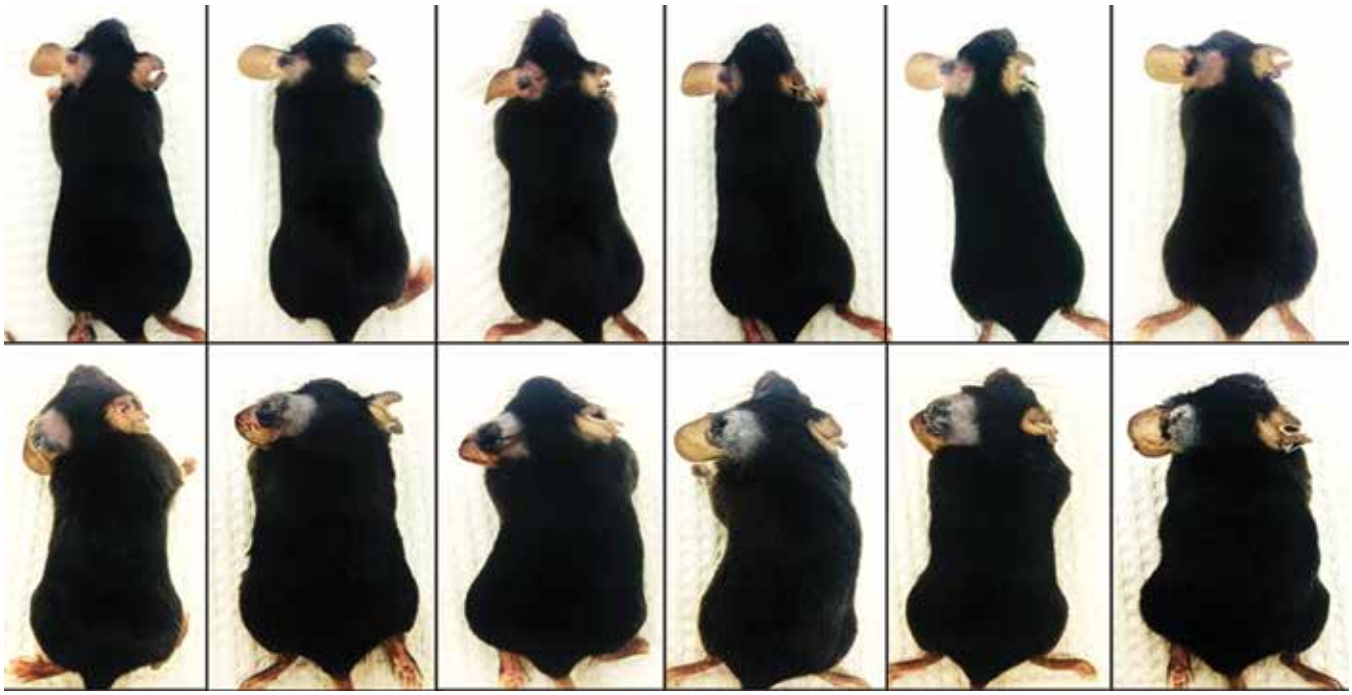

Figure 2. C57BL/6J mice transplanted in the pinna with B16F10 cells from primary tumors. Tumor morphology at euthanasia at 3 wk (top) and 4 wk (bottom) after transplantation. Tumor morphology and growth is markedly uniform in the pinna engraftment protocol after in vivo tumor cell propagation.

27-gauge needle was used for injections. Five female C57BL/6J mice were engrafted with 4×10^5 early-passage B16F10 cells propagated in cell culture as described. We engrafted 17 mice each with 4×10^5 cells in 100 µL of sterile PBS and 12 mice each with 2×10^5 cells in 100 µL of sterile PBS. Tumors were measured approximately every 7 to 10 d by using an electronic digital caliper (W80152, Performance Tool, Wilmar, Renton, WA), and tumor volumes were calculated by using the formula $\pi/6 \times \text{length} \times \text{width} \times \text{height}$. Tumors were allowed to grow to approximately 500 to 1000 mm^3 or until they began to ulcerate.

Histology. After euthanasia, all mice underwent complete, routine postmortem examination. Tumors were measured, and evidence of metastasis was recorded. Tissues including tumor, liver, lung, spleen, kidney, and mandibular lymph node were collected, fixed in 10% neutral buffered formalin, processed routinely, paraffin-embedded, sectioned at 4 µm by using a microtome, and stained with hematoxylin and eosin.

Statistical analysis. Statistical analyses were performed by using Prism 7.03 (GraphPad Software, San Diego, CA). *P* values less than 0.05 were considered significant. Differences in survival times were evaluated by generating Kaplan–Meier survival curves, and significance determined by using the log-rank test. Sigmoidal and exponential growth models were fitted by using nonlinear comparison of fits and Akaike information criteria; 95% confidence intervals of the fitted curves were graphed. Unpaired *t* tests (parametric, 2-tailed) were used to compare the high and low cell-density engraftment groups; F tests were used to determine variance.

Results

In vivo characterization of in vitro-propagated B16F10 growth and metastasis. Original experiments involved injecting B16 cells into the pinna or footpad.[6] Currently, most cancer researchers engraft B16 cells in the subcutis in the interscapular area or flank,[17,21] as is done for many transplantable models. In our experience with the B16F10 model, engraftment in this location results in marked variability in growth and morphology (Figure 1); in addition, spontaneous metastasis is not typical.

We aimed to characterize the in vivo growth kinetics of early-passage B16F10 cells. We engrafted 5 mice with 4×10^5 B16F10 murine melanoma cells in the pinna after their propagation in cell culture. Growth varied markedly between mice and was generally saltatory. One of the 5 mice (20%) did not develop a tumor over 4 wk; another animal had markedly delayed tumor

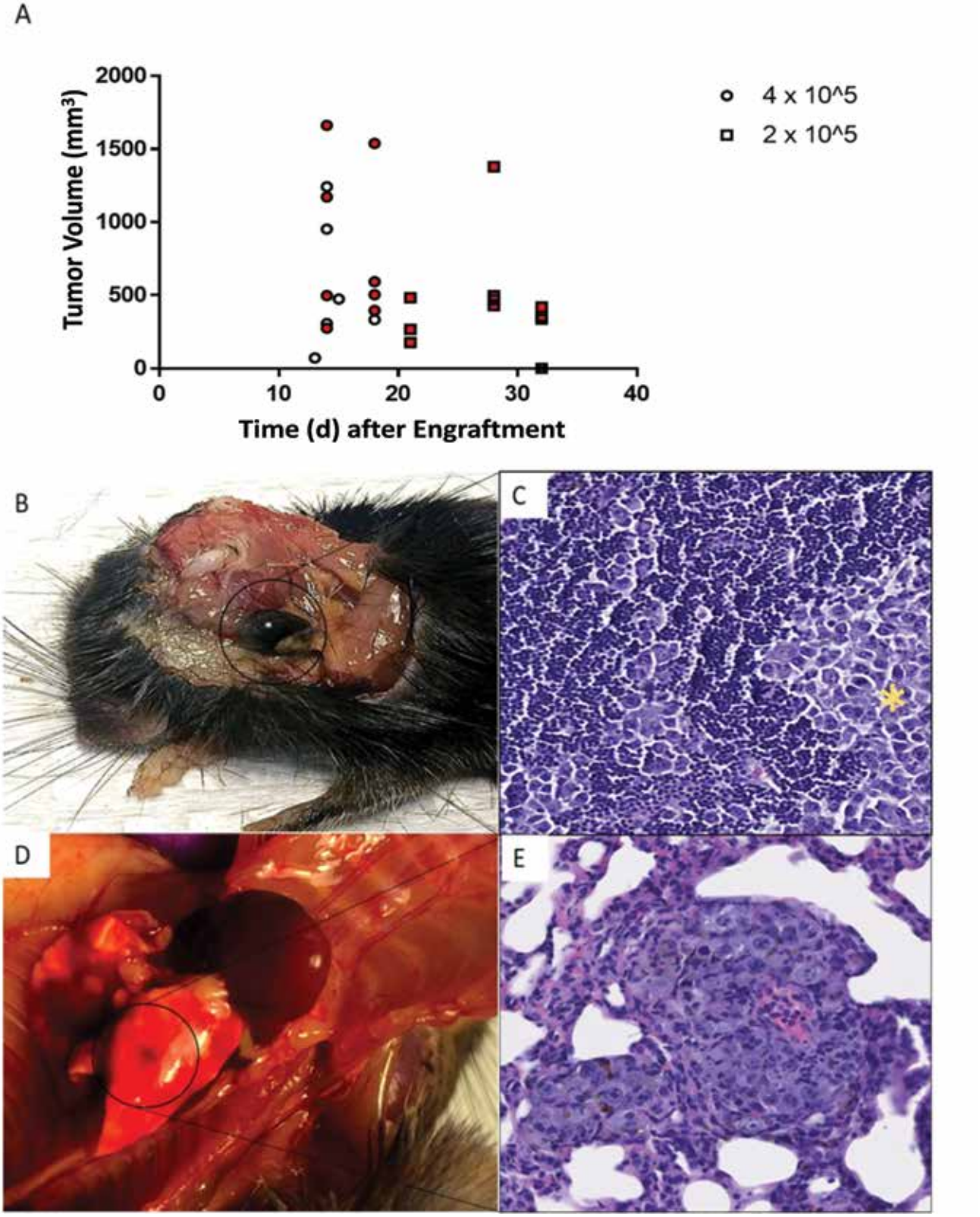

Figure 3. Melanoma tumor metastasis in mice. (A) Tumor growth of high (circles) and low (squares) cell-density engraftment over time; symbols colored red indicate that metastasis was detected. (B) Sentinel lymph node metastasis in a low cell-density–engrafted mouse. (C) Photomicrograph of sentinel lymph node metastasis (asterisk); Hematoxylin and eosin staining; magnification, 20×. (D). Focal area of lung metastasis in the left lung lobe of a low cell-density–engrafted mouse. Magnification, 10×. (E) Photomicrograph of metastatic B16F10 cells in the lungs. Hematoxylin and eosin staining.

development and did not develop a visible tumor until week 4. Among the 4 animals that developed tumors, tumor size at 3 to 4 wk varied markedly, with the smallest and largest tumors differing by almost 1000-fold. The marked variability in growth kinetics prevented the ability to fit the data to either exponential or sigmoidal mathematical growth models. Only one animal

(25%) showed evidence of spontaneous metastasis (that is, to the lungs) at postmortem examination; none of the animals had metastasis to the sentinel lymph node. The marked variability in growth rates and lag times would make tumor growth synchronization challenging for a high-throughput expanded study, and the paucity of spontaneous metastases might be problematic for researchers testing therapeutic efficacy in metastatic disease.

In vivo characterization of in vivo-propagated B16F10 growth and metastasis. Tumor cells are influenced by strong selection pressure in the tumor microenvironment.[5] One published protocol the involved a period of in vivo growth in the subcutis before engraftment in the pinna yielded spontaneous metastasis.[2,22] Therefore, we engrafted B16F10 cells in the interscapular subcutis, harvested the tumor, created a single-cell suspension, and resuspended cells in PBS before engrafting 17 animals each with 4×10^5 in vivo-propagated cells in the left pinna. All 17 animals (100%) developed a tumor (Table 1). Tumor growth generally was rapid, and a measurable tumor was present in 7 to 8 d for most animals. Mice required euthanasia between 13 and 18 d after engraftment, with the median survival time being 15 d. Evaluation of tumor volumes over time and interpolation of a standard curve showed that the growth pattern was exponential; in a nonlinear comparison of goodness-of-fit test, the probability (according to Akaike information criteria) that the exponential model was correct was 89.91%, compared with 10.09% for the sigmoidal model. In addition, at necropsy, 9 of the 17 mice had lymph node metastases (53%), and 2 of the 17 (12%) also developed lung metastasis, thus representing marked improvement over engraftment directly from cell culture.

In light of a previous study[10] that showed that the density of the cell inoculum affected the frequency of spontaneous metastasis in a murine breast cancer model using 4T1 cells, we tested whether inoculating fewer B16F10 cells increased metastasis. Therefore, we followed a similar preengraftment in vivo propagation protocol as previously, except that we engrafted mice each with approximately 2×10^5 cells (rather than 4×10^5 cells) in the left pinna. Of the 12 mice used in this experiment, 1 died unexpectedly shortly after engraftment and was therefore excluded from the analysis. Ten of the 11 remaining mice developed tumors at the site of engraftment (91% engraftment efficiency), and the tumor morphology was remarkably uniform among most mice at 3 and 4 wk (Figure 2, Table 1). The time to development of a clearly visible and measurable melanoma tumor was 3 wk.

All 10 animals that were successfully engrafted with the lower-density inoculum had gross or microscopic evidence of spontaneous metastasis to either lymph node or lung, but metastasis was primarily limited to the ipsilateral sentinel lymph node (mandibular lymph node) for most animals (Figure 3). Euthanasia was necessary between 21 and 32 d after engraftment, averaging 27 d. Of the 3 animals necropsied at 21 d (3 wk), 2 (67%) animals had evidence of spontaneous metastasis to the ipsilateral regional (mandibular) lymph node at necropsy. The third mouse had micrometastasis to the lungs (33%), but lymph node metastasis was not identified. At 28 to 32 d (4 to 4.5 wk), all 7 (100%) of the animals necropsied had metastasis to the ipsilateral mandibular lymph node, and 1 of these (14%) also had micrometastasis to the lungs.

Plotting of survival times in Kaplan–Meier curves showed that mice engrafted with a lower cell density survived longer (log-rank $P < 0.0001$; Figure 4) than those inoculated with more cells. Although mice experienced an exponential growth phase, when interpolated to a standard curve, the growth pattern using the lower cell density was a better fit for a sigmoidal model, in contrast to findings for the high cell-density–engrafted group; in a nonlinear comparison of goodness-of-fit test, the probability that the sigmoidal model was correct for the low-density inoculum was 87.91% compared with 12.09% for the exponential model (Figure 5, Table 2). These findings suggest that the improved metastatic efficiency may be related to increased survival times. The increase in survival time appears to be a function of increased lag time, but the duration of the disease once tumors became apparent did not vary significantly, regardless of the cell density of the inoculum (Table 1).

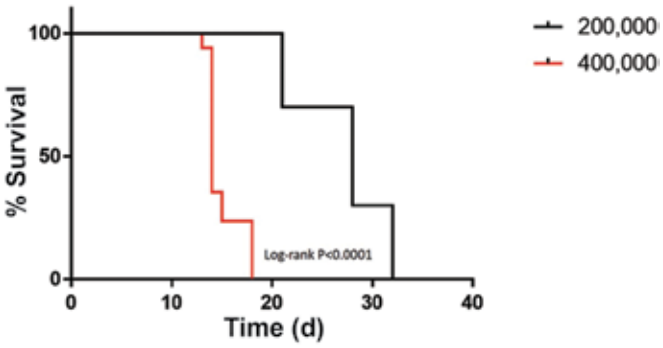

Figure 4. Kaplan–Meier survival curves comparing overall survival of mice engrafted with melanoma B16F10 cells. Overall survival times are increased in mice inoculated with lower cell doses, an effect of protracted lag times in tumor development. Log-rank $P \leq 0.0001$.

Discussion

We report here the optimization of a syngeneic mouse model system for melanoma that allows for relatively uniform growth of tumors between engrafted animals and efficient metastasis to regional lymph nodes. This model depends on the in vivo growth of B16F10 cells in the *subcutis* of mice prior to pinna engraftment, which improves tumor growth synchronization and enhances spontaneous metastasis of B16F10 murine melanoma. In addition, an inoculum of 2×10^5 cells for pinna engraftment increased lag times and enhanced metastatic efficiency.

It is generally accepted that the ideal tumor model system would exhibit predictable gross morphology, growth, and metastatic behavior.[23,27] In addition, prediction of the time of onset and incidence or engraftment rate is critical for robust, preclinical testing of early tumor stages.[18] Synchronization of tumor development is currently best achievable by using transplantable models, and the protocol we described here resulted in reasonable engraftment efficiency and synchronization in growth after in vivo propagation in the subcutis. High uniformity in morphology, growth, and spontaneous metastasis was achievable with the B16F10 murine melanoma model we described here. The observed uniform tumor morphology may at least partially reflect the engraftment site chosen. Tumor cells are less mobile when injected into the small potential space of the pinna dermis as compared with the loose interscapular subcutis, thus perhaps resulting in more consistent tumor morphology.

The pinna has been reported as a permissible site for engraftment of a wide variety of tissue types,[4] and engraftment in this location as compared with the subcutaneous tissue may be one factor in supporting tumor growth and potentiating spontaneous metastasis. The mouse pinna has a rich vascular bed. Recruitment of tumor-associated vasculature is important for tumor engraftment success and growth. In addition, the rich lymphatic supply in this region allows for easy access of neoplastic cells to lymphatic vessels, which could enhance

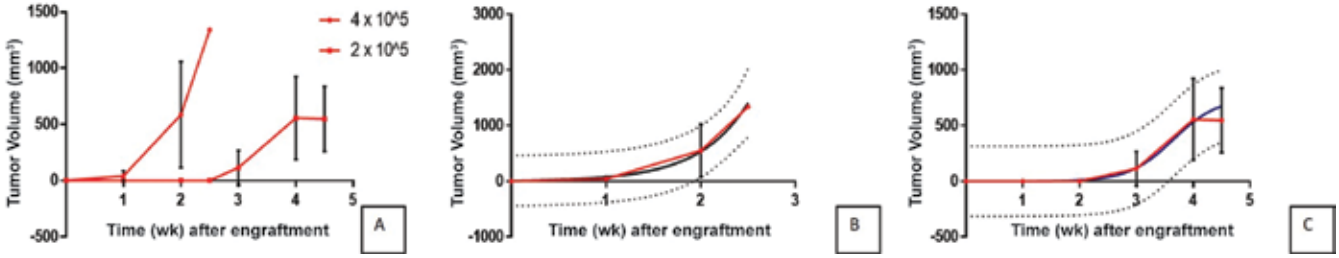

Figure 5. Fitting of in vivo growth of high and low cell-density engraftment of B16F10 cells to mathematical cell-growth models. (A) Composite of the tumor growth curves. Sigmoidal and exponential growth models were fitted by using nonlinear comparison of fits and AIC for mice engrafted with (B) 4×10^5 cells or (C) 2×10^5 cells. The red line represents the interpolated line generated by the data. The blue or black line represents the best-fit curve. Dotted lines designate the 95% confidence interval of the fitted curve. Solid points represent the mean tumor volume (bars, SEM). Specific growth rates (SGR) were calculated by using the formula ln(volume 2 / volume 1) / time 2 – time 1, and doubling times were calculated by using the formula ln2 / SGR.

Table 2. Fitting parameters of in vivo growth of B16F10 cells at different cell densities

No. of B16F10 cells inoculated	Best-fit growth model	Akaike information criteria probability	Doubling time (d)	Specific growth rate (% Δ/d)
4×10^5	Exponential	89.9%	1.7 ± 0.1	0.43 ± 0.10
2×10^5	Sigmoidal	87.9%	2.5 ± 0.4	0.40 ± 0.01

metastatic capabilities to sentinel lymph nodes (the 'anatomical–mechanical' metastasis hypothesis).[16] Spontaneous metastasis after pinna engraftment has been reported in a variety of tumor modeling protocols, including Lewis lung carcinoma and melanoma.[1,2,11,22] In addition, from a practical standpoint, monitoring of tumor growth is easier in the poorly haired area of the mouse pinna than in the heavily haired areas on the trunk. Engraftment in the poorly haired area of the pinna obviates the need for extensive or frequent shaving necessary for monitoring tumor growth in the interscapular area or flank. All of these features make the mouse pinna a favorable site for successful tumor engraftment and sustained growth and spread of tumor cells in the B16F10 murine melanoma model.

In addition, in the ideal tumor model system, tumor behavior, including metastasis, should simulate natural progression of the disease as is seen in humans. Intradermal orthotopic injection in the pinna more accurately mimics natural progression than injection directly into subcutaneous fat. The period of in vivo growth prior to transplantation to the dermis of experimental subjects may enhance local invasiveness of the tumor cells from the dermis to the subcutis and ultimately spread to lymph nodes, because tumor microenvironment can influence metastatic behavior (the 'seed and soil' metastasis hypothesis).[5] We observed that decreasing the density of the cell inoculum at engraftment increases the lag time to tumor development and overall survival times, allowing sufficient time for highly predictable, spontaneous sentinel lymph node metastasis to occur. In most mice, metastasis to the sentinel lymph node was obvious at postmortem examination. Metastasis to the sentinel lymph nodes, which is the most common first site of metastasis in humans and predictive of the entire topography of regional lymph nodes, accurately and predictably models tumor behavior in melanoma patients with stage III disease.[29]

Interestingly, a 2-fold lower cell density produced significantly higher levels of spontaneous metastasis in our mice, in agreement with the findings of authors who described the effects of inoculated cell density as a factor in growth dynamics and metastatic efficiency in a syngeneic breast cancer murine model.[10] Perhaps the general principle of decreasing cell density to enhance predictable growth and spontaneous metastasis is applicable to a wide range of transplantable syngeneic models.

Overall, tumor growth was much more predictable and uniform after cells were grown in the subcutis of a mouse before engraftment into the pinnae of other mice, and growth data could be interpolated to a standard curve, unlike for mice engrafted with in vitro propagated tumor cells. Under natural conditions, tumor growth in human patients is often observed to be saltatory,[15,24] but asynchronization can cause considerable challenges in tumor modeling and in interpreting the response to treatment in efficacy studies involving mice. There are 2 commonly argued explanations for variations in growth observed in patients over time, with neither hypothesis necessarily being mutually exclusive. One is that waves of angiogenesis and tumor infarction and necrosis cause alternating periods of adequate delivery of oxygen and nutrients, followed by periods of oxygen and nutrient deprivation resulting in undulating variation in tumor growth capacity over time.[15] The other hypothesis is that selection pressure results in the generation of mutated cells with inherently improved ability to adapt to the microenvironment and enhanced proliferative capacity; these mutant cancer cells can arise at various times resulting in marked variation in tumor growth and growth rates, even under experimental conditions.[15] Our findings are highly supportive of this 'selection pressure' hypothesis in particular. A period of preengraftment in vivo selection may help to 'preselect' for cells that are most able to adapt to the harsh conditions of the tumor microenvironment and result in more predictable growth in experimental subjects.

Reproducibility is a major challenge in preclinical oncology studies using preclinical murine tumor models. Understanding the growth kinetics and metastatic capabilities of the specific model through its optimization prior to experimentation can aid in enhancing reproducibility and improved use of existing models will contribute to improved concordance of animal studies and human patient outcomes at clinical trial. Detailed analysis and characterization of factors that affect growth kinetics and metastatic phenotype in the B16F10 murine melanoma model will aid in most efficient use of this model system. The principles we discuss here may also be relevant for other

transplantable tumor models and may have wide applicability in tumor modeling in general.

Acknowledgments

This work was supported by a grant from the Louisiana Board of Regents Governor's Biotechnology Initiative to KGK. NF was supported by the NIH training grant fellowship 2T32OD011124 "Research Training in Experimental Medicine and Pathology." We acknowledge Nithya Jambunathan for her assistance in formatting figures.

References

1. **Bobek V, Kolostova K, Pinterov D, Boubelik M, Jiang P, Yang M, Hoffman RM.** 2004. Syngeneic lymph-node–targeting model of green fluorescent protein-expressing Lewis lung carcinoma. Clin Exp Metastasis **21:**705–708. https://doi.org/10.1007/s10585-004-8118-8.
2. **Bobek V, Kolostova K, Pinterova D, Kacprzak G, Adamiak J, Kolodziej J, Boubelik M, Kubecova M, Hoffman RM.** 2010. A clinically relevant, syngeneic model of spontaneous, highly metastatic B16 mouse melanoma. Anticancer Res **30:**4799–4803.
3. **Byrne-Hoffman C,** Klinke **II** DJ**.** 2015. A quantitative systems pharmacology perspective on cancer immunology. Processes (Basel) **3:**235–256. https://doi.org/10.3390/pr3020235.
4. **Chen BJ, Jiao Y, Zhang P, Sun AY, Pitt GS, Deoliveira D, Drago N, Ye T, Liu C, Chao NJ.** 2013. Long-term in vivo imaging of multiple organs at the single-cell level. PLoS One **8:**1–9. https://doi.org/10.1371/journal.pone.0052087.
5. **Fidler IJ.** 2003. The pathogenesis of cancer metastasis: the 'seed and soil' hypothesis revisited. Nat Rev Cancer **3:**453–458. https://doi.org/10.1038/nrc1098.
6. **Fidler IJ, Nicolson GL.** 1977. Fate of recirculating B16 melanoma metastatic variant cells in parabiotic syngeneic recipients. J Natl Cancer Inst **58:**1867–1872. https://doi.org/10.1093/jnci/58.6.1867.
7. **Gershenwald JE, Colome MI, Lee JE, Mansfield PF, Tseng C, Lee JJ, Balch CM, Ross MI.** 1998. Patterns of recurrence following a negative sentinel lymph node biopsy in 243 patients with stage I or II melanoma. J Clin Oncol **16:**2253–2260. https://doi.org/10.1200/JCO.1998.16.6.2253.
8. **Gershenwald JE, Thompson W, Mansfield PF, Lee JE, Colome MI, Tseng CH, Lee JJ, Balch CM, Reintgen DS, Ross MI.** 1999. Multi-institutional melanoma lymphatic mapping experience: the prognostic value of sentinel lymph node status in 612 stage I or II melanoma patients. J Clin Oncol **17:**976–983. https://doi.org/10.1200/JCO.1999.17.3.976.
9. **Gómez-Cuadrado L, Tracey N, Ma R, Qian B, Brunton VG.** 2017. Mouse models of metastasis: progress and prospects. Dis Model Mech **10:**1061–1074. https://doi.org/10.1242/dmm.030403.
10. **Gregório AC, Fonseca NA, Moura V, Lacerda M, Figueiredo P, Simoes S, Dias S, Moreira JN.** 2016. Inoculated cell density as a determinant factor of the growth dynamics and metastatic efficiency of a breast cancer murine model. PLoS One **11:**1–19. https://doi.org/10.1371/journal.pone.0165817.
11. **Hoshida T, Isaka N, Hagendoorn J, di Tomaso E, Chen YL, Pytowski B, Fukumura D, Padera TP, Jain RK.** 2006. Imaging steps of lymphatic metastasis reveals that vascular endothelial growth factor-C increases metastasis by increasing delivery of cancer cells to lymph nodes: therapeutic implications. Cancer Res **66:**8065–8075. https://doi.org/10.1158/0008-5472.CAN-06-1392.
12. **Institute for Laboratory Animal Research.** 2011. Guide for the care and use of laboratory animals, 8th ed. Washington (DC): National Academies Press.
13. **Khanna C, Hunter K.** 2004. Modeling metastasis in vivo. Carcinogenesis **26:**513–523. https://doi.org/10.1093/carcin/bgh261.
14. **Krag DN, Meijer SJ, Weaver DL, Loggie BW, Harlow SP, Tanabe KK, Laughlin EH, Alex JC.** 1995. Minimal-access surgery for staging of malignant melanoma. Arch Surg **130:**654–658, discussion 659–660. https://doi.org/10.1001/archsurg.1995.01430060092018.
15. **Kuang Y, Nagy JD, Eikenberry SE.** 2016. Introduction to mathematical oncology. Boca Raton (FL): CRC Press.
16. **Langley RR, Fidler IJ,** 2011. The seed and soil hypothesis revisited—the role of tumor–stroma interactions in metastasis to different organs. Int J Cancer **128:** 2527–2535. https://doi.org/10.1002/ijc.26031.
17. **Mathieu V, Le Mercier M, De Neve N, Sauvage S, Gras T, Roland I, Lefranc F, Kiss R.** 2007. Galectin 1 knockdown increases sensitivity to temozolomide in a B16F10 mouse metastatic melanoma model. J Invest Dermatol **127:**2399–2410. https://doi.org/10.1038/sj.jid.5700869.
18. **Merlino G, Flaherty K, Acquavella N, Day CP, Aplin A, Holmen S, Topalian S, Van Dyke T, Herlyn M.** 2013. Meeting report: the future of preclinical mouse models in melanoma treatment is now. Pigment Cell Melanoma Res **26:**E8–E14. https://doi.org/10.1111/pcmr.12099.
19. **Morikawa K, Walker SM, Nakajima M, Pathak S, Jessup JM, Fidler IJ.** 1988. Influence of organ environment on the growth, selection, and metastasis of human colon carcinoma cells in nude mice. Cancer Res **48:**6863–6871.
20. **Morton DL, Wen DR, Wong JH, Economou JS, Cagle LA, Storm FK, Foshag LJ, Cochran AJ.** 1992. Technical details of intraoperative lymphatic mapping for early stage melanoma. Arch Surg **127:**392–399. https://doi.org/10.1001/archsurg.1992.01420040034005.
21. **Overwijk WW, Restifo NP.** 2001. B16 as a mouse model for human melanoma. Curr Protoc Immunol Chapter 20: Unit 20.1. https://doi.org/10.1002/0471142735.im2001s39
22. **Rebhun RB, Lazar AJ, Fidler IJ, Gershenwald JE.** 2008. Impact of sentinel lymphadenectomy on survival in a murine model of melanoma. Clin Exp Metastasis **25:**191–199. https://doi.org/10.1007/s10585-008-9141-y.
23. **Schuh JC.** 2004. Trials, tribulations, and trends in tumor modeling in mice. Toxicol Pathol **32 Suppl 1:**53–66. https://doi.org/10.1080/01926230490424770.
24. **Stadtländer CT.** 2016. Introduction to mathematical oncology. J Biol Dyn **10:**501–505. https://doi.org/10.1080/17513758.2016.1224937.
25. **Visonneau S, Cesano A, Torosian MH, Miller EJ, Santoli D.** 1998. Growth characteristics and metastatic properties of human breast cancer xenografts in immunodeficient mice. Am J Pathol **152:**1299–1311.
26. **Volpe JP, Milas L.** 1990. Influence of tumor transplantation methods on tumor growth rate and metastatic potential of solitary tumors derived from metastases. Clin Exp Metastasis **8:**381–389. https://doi.org/10.1007/BF01810682.
27. **Workman P, Aboagye EO, Balkwill F, Balmain A, Bruder G, Chaplin DJ, Double JA, Everitt J, Farningham DA, Glennie MJ, Kelland LR, Robinson V, Stratford IJ, Tozer GM, Watson S, Wedge SR, Eccles SA, Committee of the National Cancer Research Institute.** 2010. Guidelines for the welfare and use of animals in cancer research. Br J Cancer **102:**1555–1577. https://doi.org/10.1038/sj.bjc.6605642.
28. **Zaidi MR, Day CP, Merlino G.** 2008. From UVs to metastases: modeling melanoma initiation and progression in the mouse. J Invest Dermatol **128:**2381–2391. https://doi.org/10.1038/jid.2008.177.
29. **Zbytek B, Carlson JA, Granese J, Ross J, Mihm MC Jr, Slominski A,** 2008. Current concepts of metastasis in melanoma. Expert Rev Dermatol 3: 569–585. https://doi.org/10.1586/17469872.3.5.569.